

#### 4R.6 SIGNAL PROCESSING OF BEAM-MULTIPLEXED DATA FOR PHASED-ARRAY WEATHER RADAR

Marko B. Orešćanin<sup>(1)</sup>, Tian-You Yu<sup>(1)</sup>, Christopher D. Curtis<sup>(2)(3)</sup>, Dusan S. Zrnić<sup>(3)</sup>, and Douglas Forsyth<sup>(3)</sup>  
 (1) School of Electrical and Computer Engineering, University of Oklahoma,  
 (2) Cooperative Institute for Mesoscale Meteorological Studies (CIMMS), University of Oklahoma,  
 (3) NOAA, National Severe Storms Laboratory

##### Abstract

The S-band Phased Array Radar (PAR) has been recently installed at the National Weather Radar Testbed (NWR) in Norman, Oklahoma. It is equipped with the SPY-1A phased array antenna loaned by the NAVY and can rapidly and adaptively scan multiple regions of interest. Beam-multiplexing exploits the PAR's beam agility to provide high-quality and rapid-update weather observations. In the beam-multiplexing mode regions of interest are re-sampled after weather signals become uncorrelated. As a result, the statistical error of spectral moment estimation can be reduced optimally through the average of a number of independent measurements. Moreover, the PAR can be tasked to probe other regions during the period of re-sampling to maximize the use of radar resources. Thus the PAR can provide fast updates of weather information without compromising data quality. In this work, the feasibility and advantage of beam-multiplexing is demonstrated using numerical simulations and experimental data. Preliminary results have shown that data quality and update rate can be improved using beam-multiplexing.

#### 1. INTRODUCTION AND MOTIVATION

The time to complete a volume coverage pattern (VCP) is mainly determined by the correlation of weather signals. Conventional weather radars survey the 3D atmosphere using mechanically rotating antenna, which results in high correlation in signals from pulse to pulse. Therefore, a long dwell time is often needed to achieve the required accuracy of spectral moment estimates. On the other hand, phased array radar can mitigate the fundamental limitation of conventional radar in update time through electronic beam steering (beam-agility). Phased-array radar is able to instantaneously and adaptively control the beam position allowing novel scanning strategies based on beam-multiplexing.

#### 2. BEAM-MULTIPLEXING

The correlation coefficient of weather signals with a Gaussian power spectrum is given by the following equation (Doviak and Zrnić 1993):

$$\rho(t) = \exp\left[-8(\pi\sigma_v t / \lambda)^2\right], \quad (1)$$

where  $\sigma_v$  is the spectrum width,  $t$  is the time lag, and  $\lambda$  is the radar wavelength. An example of the correlation coefficient is shown in Figure 1 for  $\sigma_v$  of 1, 2, 3, and 4 m s<sup>-1</sup>.

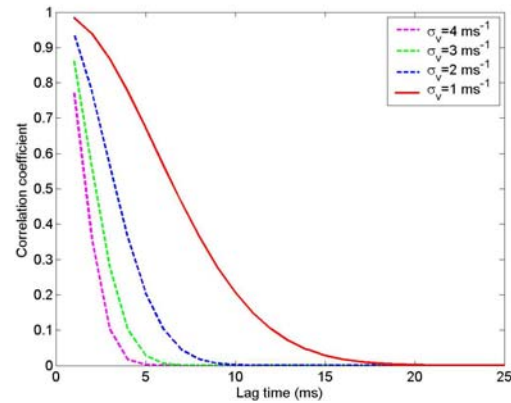


Figure 1. Correlation coefficient versus time lag

It is evident that weather signals are uncorrelated if the time between two consecutive samples is larger than 20 ms and  $\sigma_v$  is at least 1 m s<sup>-1</sup>.

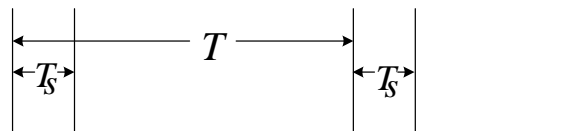


Figure 2. Independent pairs sampling

A sampling scheme of transmitting pairs of pulses separated by time  $T$  is shown in Figure 2 and is termed *independent pairs sampling* (IPS). A pair of pulses separated by  $T_s$  is transmitted in order to estimate the velocity and spectrum width. The time between pairs ( $T$ ) is typically determined by the decorrelation time of signals. If time between pairs  $T$  equals to  $T_s$  a sequence of uniformly spaced pulses is transmitted as shown in Figure 3 and is termed



Figure 3. Special case for  $T = T_s$  (Contiguous pairs sampling)

*contiguous pairs sampling* (CPS) which is used in the conventional radar. The variance of the signal power estimator for CPS is given by:

Corresponding author address: Marko B. Orešćanin  
 Rm218 202 W. Boyd St. , Carson engineering center  
 Norman, OK  
 email: orca@ou.edu

$$\text{Var}\{\hat{S}\} = \frac{S^2}{M^2} \sum_{m=-M+1}^{M-1} (M - |m|) \rho^2(mT_s) + \frac{2SN + N^2}{M}, \quad (2)$$

where  $N$  is the noise power,  $S$  is the signal power,  $\hat{S}$  is the estimated signal power,  $M$  is the number of pulses used to obtain one estimate. In a similar manner the variance of signal power for IPS is derived with the time spacing between pulse pairs taken into account. It is presented in the following equation.

$$\text{Var}\{\hat{S}\} = \frac{S^2}{L^2 M^2} \sum_{l=-(L-1)}^{L-1} (L - |l|) \rho^2(lT_s) + \sum_{m=-M+1}^{M-1} (M - |m|) \rho^2(mT) + \frac{2SN + N^2}{LM} \quad (3)$$

where  $M$  is the number of pairs of pulses and  $L=2$  is the number of pulses in each pair. Furthermore, the standard deviation (SD) of the reflectivity estimate is given by (Doviak and Zrnić 1993):

$$\sigma_z = 10 \log \left[ 1 + \frac{\sqrt{\text{Var}(\hat{S})}}{S} \right] \quad (4)$$

The SD of reflectivity for CPS and IPS is denoted by  $\sigma_{zc}$  and  $\sigma_{zi}$ , respectively.

The SD of radial velocity estimator for IPS can be represented by the following equation (Doviak and Zrnić 1993):

$$\text{SD}\{\hat{v}\} = \left[ \lambda^2 [32\pi^2 T_s^2 \rho^2(T_s)]^{-1} \{ M^{-2} [1 - \rho^2(T_s)] + \sum_{m=-(M-1)}^{M-1} \rho^2(mT) (M - |m|) + N^2 / MS^2 + (2N / MS) [1 + \rho(2T_s)(1/M - 1) \delta_{T-T_s, 0}] \} \right]^{1/2} \quad (5)$$

where  $\hat{v}$  is estimated radial velocity and  $\delta_{T-T_s} = 1$  for  $T=T_s$  and zero otherwise. Note that if  $T=T_s$  (5) applies to the CPS case.

The number of pulses needed to meet both the required SD of 1 dB and  $1 \text{ m s}^{-1}$  for reflectivity and velocity, respectively, can be derived using (2), (3), (4) and (5). The results for both IPS and CPS are shown in Figure 4 for SNR = 20 dB, where an average of four reflectivity estimates in range is considered. In the IPS case  $\sigma_{zi}$  governs the required number of samples for  $\sigma_v$  from 1 to approximately  $1.5 \text{ m s}^{-1}$ , while the SD of velocity dominates the number of pulses at larger spectrum width. Similarly, for CPS the SD of velocity becomes a dominant factor at approximately  $\sigma_v = 2.6 \text{ m s}^{-1}$ . A larger number of pulses is needed for CPS to reduce the SD of reflectivity estimates at smaller spectrum widths than the one for IPS. It is due to the large correlation between samples (as can be seen from (1) and (2)).

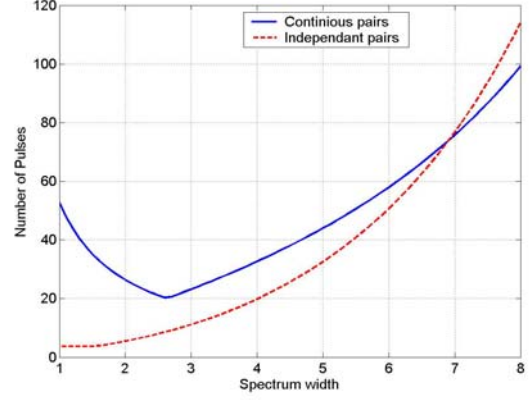


**Figure 4.** Number of pulses needed to meet standard deviation limits at SNR = 20 dB.

The number of pulses need to meet the 1 dB SD of reflectivity estimate is small at large  $\sigma_v$  because of the low correlation between samples. At the same time, however, more pulses is needed to meet the required velocity accuracy because large signal correlation is required in the pulse-pair velocity estimation. At small  $\sigma_v$  estimation of reflectivity is improved significantly using IPS through an average of more equivalent independent measurements over pairs. The SD of the velocity is determined by  $M$ ,  $\rho(T_s)$  and  $\rho(T)$  as shown in (5) and (1). For lower  $\sigma_v$ , the SD of the velocity is governed by the correlation within a pair  $\rho(T_s)$ . Consequently,  $\text{SD}(\hat{v})$  increases with  $\sigma_v$ , which can be observed in Figure 4 as an increase in number of pulses. For large  $\sigma_v$  correlation among samples is low so the primary factor that affects  $\text{SD}(\hat{v})$  is the number of pairs  $M$ . For example, let us consider a case when a number of 32 pulses is transmitted using both CPS and IPS. As a result, the available pairs used to estimate one velocity for CPS and IPS are 31 and 16, respectively. In other words, IPS requires more samples than CPS to meet the required  $\text{SD}(\hat{v})$ . This crossover is evident in Figure 4 and indicates that CPS should be used when  $\sigma_v$  is larger than  $7 \text{ m s}^{-1}$ . In this case, the PAR can transmit a sequence of contiguous pulses (all separated in time by  $T_s$ ) at a fixed radial position and steer discretely to the next one. This sampling scheme can still achieve better performance because the effect of beam broadening caused by the antenna motion is avoided.

Three constraints will be considered when the beam multiplexing strategy is designed:

1. The shortest time period between collection of two consecutive samples must be at least 20 ms.
2. Sufficient separation between two subsequent beam positions is needed in order to mitigate the second and third trip echoes (Curtis, 2002). This is primarily determined by the radar beamwidth

3. In order to estimate three spectral moments a pair of pulses is transmitted at each beam position with a specified PRT between the pulses.

As a result, a cell of  $14^\circ$  sector scanned using beam-multiplexing was designed and is depicted in Figure 5. The  $14^\circ$  sector in azimuth (from  $0^\circ$  to  $13^\circ$ ) is scanned with 14 beam positions. In addition, the consecutive beam positions are separated by at least  $6^\circ$  to mitigate the second and third trip echo. Position No. 1 ( $P[1]$ ) is at  $0^\circ$ , the position No. 2 ( $P[2]$ ) is at  $7^\circ$  in azimuth,  $P[3]$  is at  $1^\circ$ ,  $P[4]$  is at  $8^\circ$  and so forth. This makes for the  $7^\circ$  distance in azimuth between each two  $P[2k-1]$  and  $P[2k]$  positions (where  $k = 1 \dots 7$ ). At the same time, the distance between positions  $P[2k]$  and  $P[2k+1]$  is  $6^\circ$  in azimuth. Two pulses are transmitted at every beam position. This pattern is repeated until desired number of pulses is sent at every position. For instance in order to collect 16 pulses at every position this scanning scheme will be repeated 8 times.

The other scanning scheme is to mimic contiguous scanning, and is depicted in Figure 6. Position No. 1 ( $P[1]$ ) is at  $0^\circ$ , the position No. 2 ( $P[2]$ ) is at  $1^\circ$  in azimuth,  $P[3]$  is at  $2^\circ$ ,  $P[4]$  is at  $3^\circ$  and so forth. Desired number of pulses is transmitted in sequence at every position.

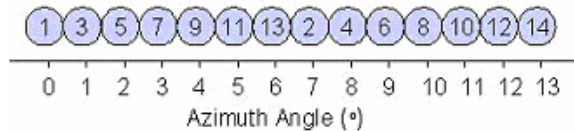


Figure 5. Beam-Multiplexing scanning cell

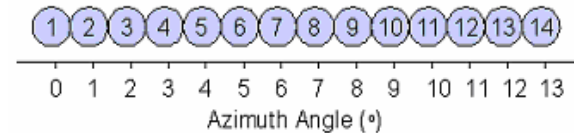


Figure 6. Mimicking contiguous scanning

### 3. EXPERIMENT AND RESULTS

An experiment was designed to demonstrate the feasibility of beam multiplexing and to compare it with the conventional scanning strategy. A sector of  $28^\circ$  in azimuth was scanned using the two following strategies. The first scanning strategy was constructed using two beam multiplexing cells, each with a  $14^\circ$  coverage as shown in Figure 5. The second strategy mimics contiguous scanning (Figure 6), but with fixed beam positions in azimuth separated by 1 degree covering a  $28^\circ$  scan. At every beam position 64 pulses were transmitted for both strategies. In other words, the same time of  $64 \cdot 28 \cdot 1 \text{ms} = 1.792 \text{ s}$  is required for both strategies to cover the  $28^\circ$  sector. Both scanning strategies were repeated 50 times.

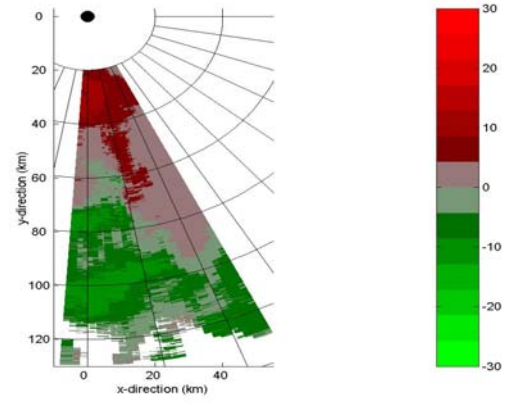


Figure 7. Velocity from Beam-Multiplexing

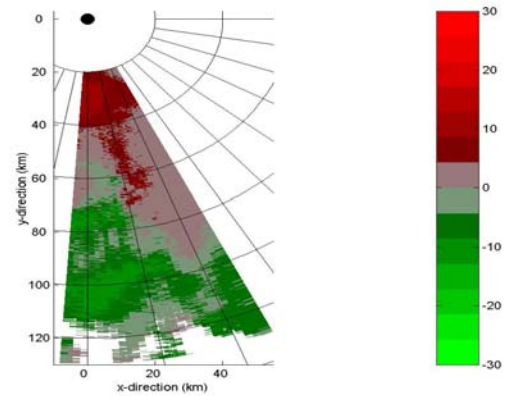


Figure 8. Velocity from Contiguous scanning

The experiment was conducted on May 2<sup>nd</sup>, 2005 starting at 15:07:5 UTC. The PAR operates at a frequency of 3.2 GHz. PRT and pulse width are 1 ms and 1.57  $\mu\text{s}$ , respectively. The sampling frequency was 2.5 MHz which resulted in range oversampling with a factor of 4. This provides a potential for further improvement of the performance using the whitening technique (Torres and Zrnić 2003; Ivić et al 2003).

The velocity fields from both strategies are presented in Figures 7 and 8 for one scan. The radar is located at the origin. It is apparent that the velocity fields are extremely similar. However, the shape of the features with velocities around  $5 \text{ m s}^{-1}$  (between 17 km and 22 km in the x-direction and between 40 km and 60 km in the y-direction) are slightly different.

Over the 50 scans the statistical mean and the SD of the three spectral moments are analyzed. The mean reflectivity and velocity at azimuth of  $165^\circ$  are shown in Figures 9 and 10, respectively. It is evident that both mean fields agree extremely well. Furthermore, the SD of the reflectivity and velocity at azimuth angle of  $165^\circ$  is shown in Figures 11 and 12, respectively. The temporal variation in weather was removed by linearly fitting the data over the 50 realizations.

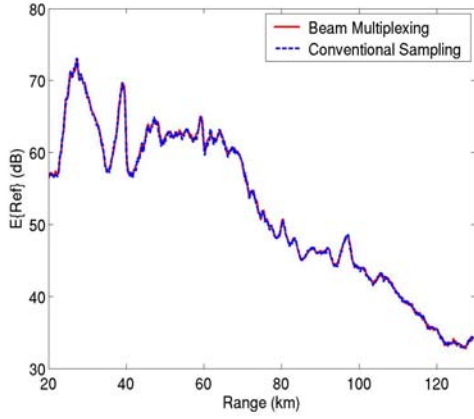


Figure 9. Mean Reflectivity

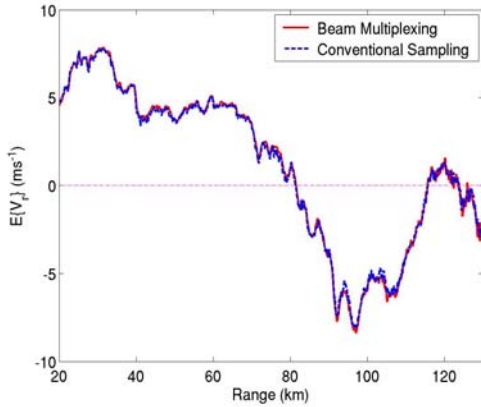


Figure 10. Mean Velocity

In Figure 11 a SD of reflectivity estimates obtained from beam-multiplexed data (IPS) is consistently smaller than the SD of reflectivity from CPS data. Reduction of SD in reflectivity estimates is most evident in the region between 20 and 75 km, where the SNR is at least 20 dB and the spectrum width is approximately 1-3 m s<sup>-1</sup>. When  $\sigma_v$  is low (the correlation of signals is high) decreasing the number of independent samples  $M_i$  resulting in a higher variance for power estimates. CPS is more affected by this than IPS due to the fact that in IPS we have only correlation within a pair of pulses and there is no correlation between the pulse-pairs, thus implying the lower variance levels for the IPS. On the other hand, the reduction of SD is limited in range between 75 km and 110 km where the larger  $\sigma_v$  (3ms<sup>-1</sup> to 4.5 ms<sup>-1</sup>) and the lower SNR (20 to 5 dB) are observed. With the increase in  $\sigma_v$  the autocorrelation among samples decreases resulting in the reduced variances in power estimates. Consequently, the improvement from IPS is degraded.

In Figure 12 the SD of velocity estimates is presented together with the SNR and the mean spectrum width. Additionally, two theoretical curves obtained using (5) for both independent and contiguous pairs sampling are superimposed. With SNR of at least 20 dB region of interest is between 20 km and 75 km. In this region  $\sigma_v$  is 1-3 m s<sup>-1</sup>. The SD of the velocity estimates are

fairly small due to the lower  $\sigma_v$ . As in power estimates, the reduction

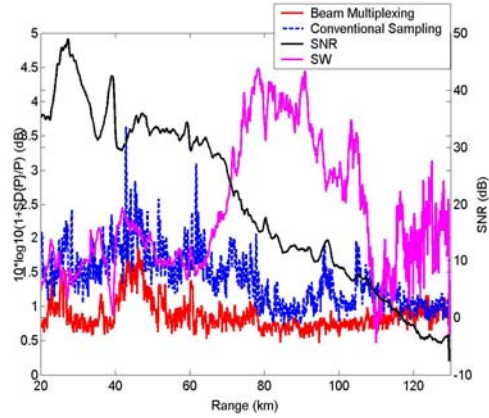


Figure 11. Standard Deviation of Reflectivity

of the velocity SD for beam-multiplexing can be observed in this region. Moreover, the SD obtained from theoretical derivation and experimental data agree well for both IPS and CPS schemes. It can also be observed that for low SNR there is a cross-over of two SD curves (Range 110 km), also expected from theoretical prediction (Figure 6.5 in Doviak and Zrnić 1993).

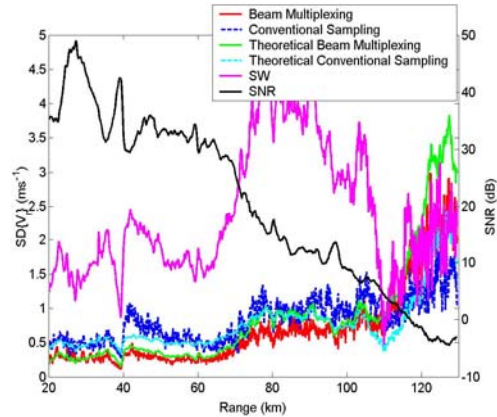


Figure 12. Standard Deviation of Velocity

#### 4. CONCLUSIONS

Improved quality of samples and faster scanning rates are two contradictory demands that mechanically steered radar antennas cannot meet. Electronically scanned antennas offer a possibility to mitigate this limitation.

Beam-Multiplexing can be integrated with techniques for improving the variance of estimates such as whitening (Torres and Zrnić 2003). For  $K$ -times oversampled data in range, the reduction of standard deviation would be  $K^{1/2}$  which combined with the reduction of  $(M_i)^{1/2}$  ( $M_i$  number of independent samples) introduced by beam-multiplexing would give the total reduction in standard deviation of  $(KM_i)^{1/2}$ . In this particular case for  $K=4$  and  $M_i=4$ , this would result in a reduction of  $(KM_i)^{1/2}=4$ . This considerable

reduction in standard deviation can be transformed into the improvement in update time by a factor of 4.

#### **ACKNOWLEDGEMENT**

M. B. Orešćanin is grateful for the support of this research provided by the National Severe Storms Laboratory (NSSL) and Cooperative Institute for Mesoscale Meteorological Studies (CIMMS)

#### **REFERENCES**

- Curtis C., 2002: National Weather Radar Testbed, Technical report NSSL
- Doviak, R. J. and D. S. Zrnica, 1993: Doppler radar and weather observations, 2nd ed., Academic Press, Inc., 562 pp
- Doviak, R. J., D. S. Zrnica, and A. Shapiro, 2001: Phased array weather radar-benefits and challenges. *Preprints*, 30th International Conference on Radar Meteorology, Munich, Germany, Amer. Meteor. Society, 202-204.
- Ivic, R. I., D. S. Zrnica, Torres M. S., 2003: Whitening in range to improve weather radar spectral moment estimates. Part II: Experimental Evaluation. *J. Atmos. Oceanic Technol.*, **20**, 1449-1459.
- Torres M. S. and D. S. Zrnica, 2003: Whitening in range to improve weather radar spectral moment estimates. Part I: Formulation and Simulation. *J. Atmos. Oceanic Technol.*, **20**, 1433-1448.